



Cite this: *Polym. Chem.*, 2015, **6**, 4436

# Construction of regio- and stereoregular poly(enaminone)s by multicomponent tandem polymerizations of diynes, diacyl chloride and primary amines†

Haiqin Deng,<sup>a,b</sup> Rongrong Hu,<sup>a,c</sup> Anakin C. S. Leung,<sup>a,b</sup> Engui Zhao,<sup>a,b</sup> Jacky W. Y. Lam<sup>\*a,b</sup> and Ben Zhong Tang<sup>\*a,b,c</sup>

Polyhydroaminations for the synthesis of stable nitrogen-substituted conjugated polymers with well-defined structures remain a great challenge and the control of the regio- and stereochemistry of the enamine product of the hydroamination is non-trivial. Herein we report an efficient tandem polymerization of alkynes, carbonyl chlorides and primary amines to afford regio- and stereoregular conjugated poly(enaminone)s. The atom-economical one-pot sequential polycondensation–hydroamination polymerization catalyzed by Pd(PPh<sub>3</sub>)<sub>2</sub>Cl<sub>2</sub>/CuI proceeded smoothly under mild conditions, furnishing nitrogen-substituted conjugated polymers with high molecular weights (up to 46 100) and high regio-/stereoregularities (100%) in nearly quantitative yields (up to 99%). The single crystal structure of the model compound, together with the NMR spectra comparison of the model compound and polymers provided direct insight into the stereoselectivity of the polymerization, verifying the sole *Z*-vinylene isomer of the polymers. Through the exquisite structural design strategy of the intramolecular hydrogen bond of the resulting hydroamination product, the tautomerization between enamine and imine as well as *E/Z* isomerization was successfully avoided, providing products with high chemical stability and sole *Z*-vinylene isomers. The conjugated polymers display excellent solubility in common organic solvents, good film-forming ability, and high thermal stability. The hydrogen bond formation of the polymer helps to block the potential photo-induced electron transfer process and the polymer shows a unique aggregation-enhanced emission phenomenon: their solutions are weakly emissive, while their nanoaggregates or thin films are brightly emissive. Furthermore, thin films of the polymers enjoy high refractive indices (1.9103–1.6582) in a wide wavelength region of 400–1000 nm, which can be further modulated by UV irradiation. Meanwhile, well-resolved fluorescent photopatterns of the polymers can be fabricated through the UV irradiation of thin films *via* a copper photomask.

Received 30th March 2015,

Accepted 10th May 2015

DOI: 10.1039/c5py00477b

[www.rsc.org/polymers](http://www.rsc.org/polymers)

<sup>a</sup>Department of Chemistry, Institute for Advanced Study, Institute of Molecular Functional Materials, Division of Biomedical Engineering, Division of Life Science and State Key Laboratory of Molecular Neuroscience, The Hong Kong University of Science & Technology (HKUST), Clear Water Bay, Kowloon, Hong Kong.

E-mail: [chjacky@ust.hk](mailto:chjacky@ust.hk), [tangbenz@ust.hk](mailto:tangbenz@ust.hk)

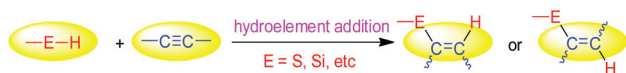
<sup>b</sup>HKUST-Shenzhen Research Institute, No. 9 Yuexing 1st RD, South Area, Hi-tech Park, Nanshan, Shenzhen 518057, China

<sup>c</sup>Guangdong Innovative Research Team, SCUT-HKUST Joint Research Laboratory, State Key Laboratory of Luminescent Materials and Devices, South China University of Technology (SCUT), Guangzhou 510640, China

† Electronic supplementary information (ESI) available: Crystal data and structure refinement for model compound **4**; frontier orbital theory for the PET effect; quantum yields of **4** and P1a–b/2/3a–b in the solution and aggregate state. CCDC 1009262. For ESI and crystallographic data in CIF or other electronic format see DOI: 10.1039/c5py00477b

## Introduction

The construction of functional macromolecules is of great academic significance and technological implication, and has attracted much attention among scientists.<sup>1</sup> As an important branch, heteroatom-containing conjugated polymers are in great demand in many potential high-tech applications, attributed to their unique electronic and photophysical properties.<sup>2</sup> Various polymerization methods towards heteroatom-containing conjugated polymers have been developed over the past few decades, and hetero-elements such as sulfur, oxygen, nitrogen, silicon, are normally incorporated into the polymer structures.<sup>3</sup> However, the exploration of facile polymerization methodologies to afford regio- and stereoregular products remains challenging.<sup>4</sup>



**Scheme 1** Hydroelement additions of alkynes.

Among many polymerization approaches, hydroelement addition reactions of alkynes are considered to be one of the most efficient methods to construct conjugated polymers with  $\sigma$ - $\pi$  conjugation (Scheme 1).<sup>5</sup> Some frontier work about polyhydroelement additions has been reported. For example, linear and hyperbranched poly(silylenevinylene)s were synthesized by polyhydrosilylations of alkynes and silanes.<sup>6</sup> Furthermore, polyhydrothiolations of aromatic diynes and dithiols catalyzed by rhodium complexes,<sup>7</sup> and catalyst-free polyhydrothiolations were reported,<sup>8</sup> which proceeded smoothly in a regioselective manner, affording conjugated poly(vinylene sulfide)s. In the reported polyhydrosilylations and polyhydrothiolations, despite that high stereoselectivities were reported in some cases,<sup>6</sup> both *Z*-vinylene and *E*-vinylene isomers were generally observed in the obtained polymers.

Polyhydroaminations with direct addition of amines to alkynes, however, are rarely reported, probably due to the poor stability of the addition product. Of the reported small molecular hydroamination reactions,<sup>9</sup> there lies one critical issue which limits the development of hydroaminations. As shown in Scheme 2, the tautomerization between enamine and imine takes place easily, and the C=N bond in imine is unstable which can be decomposed.<sup>10</sup> Meanwhile, the stereoselectivity of the newly formed C=CH bond is difficult to control. It is thus a great challenge to synthesize nitrogen-substituted conjugated polymers with well-defined structures through polyhydroaminations.

To develop polymerization methods with operational simplicity, synthetic efficiency, high atom economy, and environmental benefit, scientists have made great endeavor to investigate multicomponent polymerizations (MCPs),<sup>11</sup> including the MCPs of alkynes, aldehydes and amines,<sup>12</sup> and the MCPs of alkynes, azides and amines/alcohols.<sup>13</sup> In our previous work, multicomponent tandem polymerizations (MCTPs) with maximization of the reaction efficiency and atom/step-economy have been developed, which include sequential or cascade reaction processes. For example, a one-pot, three-component, coupling-hydrothiolation-cyclocondensation MCTP of the alkyne, aryl chloride, and ethyl 2-mercaptoacetate was explored as a powerful tool for the preparation of conjugated poly(arylene thiophenylene) with structural regularity, processability and advanced functionality.<sup>14</sup> To explore



**Scheme 2** Hydroamination reaction and enamine-imine tautomerization.

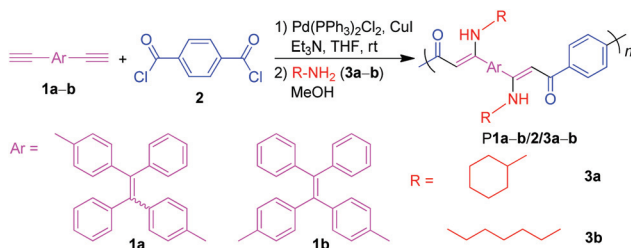
the general applicability of this MCTP, the one-pot, two-step, three-component coupling-addition tandem polymerizations of alkynes, aryl chlorides, and common aliphatic/aromatic thiols are investigated, demonstrating an efficient polymerization method to access sulfur-substituted conjugated polymers.<sup>15</sup>

Encouraged by the successful development of MCTPs of alkynes, aryl chlorides, and thiols through combining Sonogashira coupling and hydrothiolation, it is promising to extend this concept by using amines instead of thiols to develop sequential coupling-hydroamination polymerizations. In fact, Müller *et al.* reported an economical and practical protocol for the one-pot three-component coupling-addition sequential reaction of alkynes, carbonyl chlorides and primary amines, using Pd(PPh<sub>3</sub>)<sub>2</sub>Cl<sub>2</sub>/CuI as a catalyst to afford enaminoone with high efficiency, yielding a sole *Z*-isomer product due to the formation of an intramolecular hydrogen bond (Scheme 3).<sup>16</sup> The six-membered ring linked by the intramolecular hydrogen bond between N-H and C=O groups can help to stabilize the *Z*-vinylene structure, avoiding tautomerization between enamine and imine and *E/Z* isomerization, inducing high stereoselectivity, and hence providing perfect solution to the unsolved problems of polyhydroaminations.

In this work, a one-pot three-component coupling-hydroamination sequential polymerization was developed to afford nitrogen-substituted conjugated polymers with regio- and stereoregular structures. Tetraphenylethene (TPE) was incorporated into the monomer structures because it is a well-known aggregation-induced emission (AIE) fluorophore.<sup>17</sup> The restriction of intramolecular motion was proposed as the main reason for the AIE effect of TPE derivatives.<sup>18</sup> In solution, the phenyl rings can rotate *via* the single-bond axis, which serves as a relaxation channel for the decay of excitons, rendering the TPE molecules nonemissive. In the aggregated state, however, such rotation is physically restricted, blocking the nonradiative decay pathway, which enables the molecules with bright emission. The introduction of TPE units may thus endow the polymers with aggregation-enhanced emission (AEE) features. The bulky and twisted structure of TPE units can also prevent close intermolecular interactions, which presumably benefits the solubility of the resulting polymers. The sequential polymerizations of TPE-containing diynes (**1a-b**), diaryl chloride (**2**) and primary amines (**3a-b**) (Scheme 4) can proceed smoothly to furnish stereospecific conjugated polymers (**P1a-b/2/3a-b**) with satisfactory molecular weights (*M<sub>w</sub>*) in nearly quantitative yields. The resulting polymers possess good chemical stability, excellent solubility, good thermal stability, aggregation-enhanced emission, high light refractivity, as well as photopatternability.



**Scheme 3** One-pot enaminone syntheses by coupling-addition of alkynes, aryl chlorides and primary amines.



**Scheme 4** Polymerizations of diynes **1a–b**, carbonyl chloride **2**, and primary amines **3a–b**.

## Results and discussion

### Polymerization

To develop the one-pot three-component sequential coupling–hydroamination reaction into an efficient polymerization approach for the preparation of conjugated poly(enaminone)s, monomers with multiple functional groups were designed. TPE-containing diynes **1a–b** were prepared according to our previous publications.<sup>19</sup> Commercially available terephthaloyl chloride **2** and primary amines **3a–b** were chosen as the other two monomers. The typical polymerization was carried out in THF under nitrogen in the presence of Pd(PPh<sub>3</sub>)<sub>2</sub>Cl<sub>2</sub>, CuI and triethylamine (Et<sub>3</sub>N). Diynes **1a–b** were first reacted with dicarbonyl chloride **2** for 15 min at room temperature, **3a–b** were then added with methanol for the hydroamination reaction to proceed, affording nitrogen-substituted conjugated polymers (Scheme 4).

The temperature effect of the hydroamination was first evaluated with the polymerization of **1a**, **2**, and **3a** as shown in Table 1. The polymerization was first carried out at room temperature for 6 h; only a trace amount of the target polymer was obtained. Prolonging the reaction time to 14 h did not improve the polymerization and few desired polymeric products were generated in the system. The reaction temperature of hydroamination was then increased to 80 °C. After 6 h of polymerization, a polymer with a high *M<sub>w</sub>* of 40 800 was obtained in a high yield of 99%. High temperature is hence necessary for the hydroamination process and further optimizations of the polymerization were carried out at 80 °C.

**Table 1** Temperature effect on the polymerization of **1a**, **2** and **3a**<sup>a</sup>

No.	<i>T</i> (°C)	<i>t</i> (h)	Yield (%)	<i>M<sub>w</sub></i> <sup>b</sup>	<i>M<sub>w</sub>/M<sub>n</sub></i> <sup>b</sup>
1 <sup>c</sup>	25	6	/		
2 <sup>c</sup>	25	14	/		
3	80	6	99	40 800	2.3

<sup>a</sup> Carried out in THF under nitrogen in the presence of Pd(PPh<sub>3</sub>)<sub>2</sub>Cl<sub>2</sub>, CuI and Et<sub>3</sub>N. [**1a**] = 0.05 M, [**2**] = 0.05 M, [**3a**] = 0.20 M, [Pd] = 4 mol%, [Cu] = 8 mol%, [Et<sub>3</sub>N] = 0.10 M. Monomer **1a** was reacted with **2** for 15 min at room temperature prior to the addition of **3a**. <sup>b</sup> *S* = solubility tested in common organic solvents such as THF, DCM, and chloroform: √ = completely soluble and Δ = partially soluble. <sup>c</sup> Determined by GPC in THF on the basis of a linear polystyrene calibration. <sup>c</sup> Undesired polymeric products were obtained.

**Table 2** Solvent effect on the polymerization of **1a**, **2** and **3a**<sup>a</sup>

No.	Solvents	Yield (%)	<i>M<sub>w</sub></i> <sup>b</sup>	<i>M<sub>w</sub>/M<sub>n</sub></i> <sup>b</sup>
1	DCM/methanol	Trace		
2	DMF/methanol	Trace		
3	Toluene/methanol	97	30 400	1.4
4 <sup>c</sup>	THF/methanol	99	40 800	2.3

<sup>a</sup> Carried out in the solvents under nitrogen at 80 °C in the presence of Pd(PPh<sub>3</sub>)<sub>2</sub>Cl<sub>2</sub>, CuI and Et<sub>3</sub>N. [**1a**] = 0.05 M, [**2**] = 0.05 M, [**3a**] = 0.20 M, [Pd] = 4 mol%, [Cu] = 8 mol%, [Et<sub>3</sub>N] = 0.10 M. Monomer **1a** was reacted with **2** for 15 min at room temperature prior to the addition of **3a**, DMF = dimethyl formamide. <sup>b</sup> Determined by GPC in THF on the basis of a linear polystyrene calibration. <sup>c</sup> Data taken from Table 1, no. 3.

The solvent effect of the polymerization was then systematically investigated (Table 2). Of the tested solvents including DCM, DMF, toluene, and THF, THF presents as the most suitable medium for the polymerization, giving a soluble polymeric product with the highest *M<sub>w</sub>* and yield (Table 2, no. 4). Satisfactory results were also obtained in toluene with a high *M<sub>w</sub>* of 30 400, low polydispersity (*M<sub>w</sub>/M<sub>n</sub>* = 1.4), and a high yield of 97%. However, only a trace amount of the polymeric product was produced in DCM or DMF, indicating a strong solvent effect of the polymerization.

The reaction time of the hydroamination after the addition of **3a** and methanol was then tested in THF. As shown in Table 3, the polymerization is very efficient. In general, with the second step reaction time ranging from 2 to 24 h, the yields of P**1a/2/3a** were excellent which remained almost constant (~98%), and the *M<sub>w</sub>* values of the polymers were generally larger than 36 000. The polymers obtained after 12 h and 24 h became partially soluble in common organic solvents.

The influence of the monomer concentrations on the polymerization was also investigated (Table 4). When the concentrations of **1a** and **2** were both 0.10 M, an insoluble gel was rapidly formed within 2 h. The concentrations of **1a** and **2** were then decreased to 0.08 M, while keeping [**1a**]:[**2**]:[**3a**] = 1:1:4, a partially soluble polymer was produced in high yield. The best polymerization result was achieved with a monomer

**Table 3** Time course on the polymerization of **1a**, **2** and **3a**<sup>a</sup>

No.	<i>t</i> (h)	Yield (%)	<i>S</i> <sup>b</sup>	<i>M<sub>w</sub></i> <sup>c</sup>	<i>M<sub>w</sub>/M<sub>n</sub></i> <sup>c</sup>
1	2	99	√	36 400	2.3
2	4	99	√	46 100	2.9
3 <sup>d</sup>	6	99	√	40 800	2.3
4	12	99	Δ	42 100	3.0
5	24	98	Δ	41 800	3.2

<sup>a</sup> Carried out in THF under nitrogen at 80 °C in the presence of Pd(PPh<sub>3</sub>)<sub>2</sub>Cl<sub>2</sub>, CuI and Et<sub>3</sub>N. [**1a**] = 0.05 M, [**2**] = 0.05 M, [**3a**] = 0.20 M, [Pd] = 4 mol%, [Cu] = 8 mol%, [Et<sub>3</sub>N] = 0.10 M. Monomer **1a** was reacted with **2** for 15 min at room temperature prior to the addition of **3a**. <sup>b</sup> *S* = solubility tested in common organic solvents such as THF, DCM, and chloroform: √ = completely soluble and Δ = partially soluble. <sup>c</sup> Determined by GPC in THF on the basis of a linear polystyrene calibration. <sup>d</sup> Data taken from Table 1, no. 3.

**Table 4** Monomer concentration on the polymerization of **1a**, **2** and **3a**<sup>a</sup>

No.	[ <b>1a</b> ] (M)	<i>t</i> (h)	Yield (%)	<i>S</i> <sup>b</sup>	<i>M</i> <sub>w</sub> <sup>c</sup>	<i>M</i> <sub>w</sub> / <i>M</i> <sub>n</sub> <sup>c</sup>
1	0.10	2	Gel			
2	0.08	6	96	Δ	20 200	2.5
3 <sup>d</sup>	0.05	6	99	√	40 800	2.3
4	0.02	6	43	√	13 400	2.3

<sup>a</sup> Carried out in THF under nitrogen at 80 °C in the presence of Pd(PPh<sub>3</sub>)<sub>2</sub>Cl<sub>2</sub>, CuI and Et<sub>3</sub>N for 6 h. [**2**] = [**1a**], [**3a**] = 4 [**1a**], [Et<sub>3</sub>N] = 2 [**1a**], [Pd] = 4 mol%, [Cu] = 8 mol%. Monomer **1a** was reacted with **2** for 15 min at room temperature prior to the addition of **3a**. <sup>b</sup> *S* = solubility tested in common organic solvents such as THF, DCM, and chloroform: √ = completely soluble and Δ = partially soluble. <sup>c</sup> Determined by GPC in THF on the basis of a linear polystyrene calibration. <sup>d</sup> Data taken from Table 1, no. 3.

**Table 5** Polymerization of **1a–b**, **2** and **3a–b**<sup>a</sup>

No.	Monomer	Yield (%)	<i>M</i> <sub>w</sub> <sup>b</sup>	<i>M</i> <sub>w</sub> / <i>M</i> <sub>n</sub> <sup>b</sup>
1 <sup>c</sup>	<b>1a/2/3a</b>	99	40 800	2.3
2	<b>1b/2/3a</b>	99	21 400	2.2
3	<b>1a/2/3b</b>	95	25 200	2.0

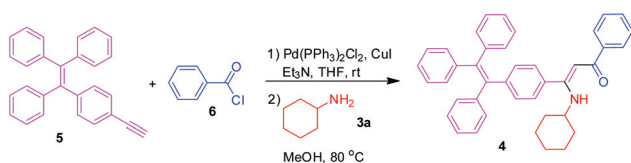
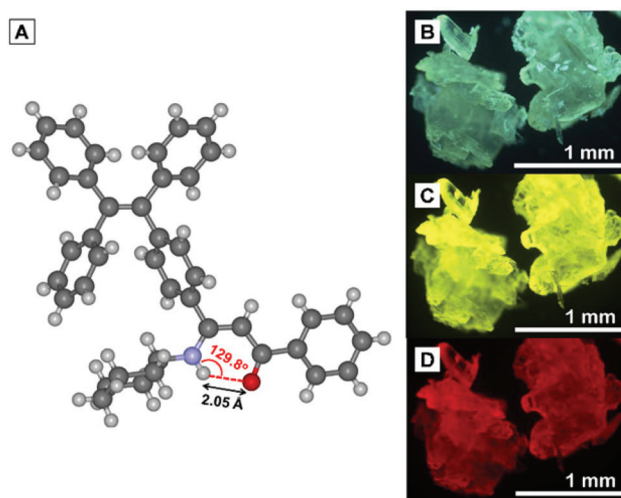
<sup>a</sup> Carried out in THF under nitrogen at 80 °C in the presence of Pd(PPh<sub>3</sub>)<sub>2</sub>Cl<sub>2</sub>, CuI and Et<sub>3</sub>N for 6 h. [**1a**] = [**1b**] = [**2**] = 0.05 M, [**3a**] = [**3b**] = 0.20 M, [Pd] = 4 mol%, [Cu] = 8 mol%, [Et<sub>3</sub>N] = 0.10 M. Monomer **1a/1b** was reacted with **2** for 15 min at room temperature prior to the addition of **3a/3b**. <sup>b</sup> Determined by GPC in THF on the basis of a linear polystyrene calibration. <sup>c</sup> Data taken from Table 1, no. 3.

concentration of 0.05 M. Further dilution of the monomers to 0.02 M led to a dramatically decreased yield and *M*<sub>w</sub>.

Last but not least, other monomer structures were tested under the optimum conditions to explore the general applicability of this polymerization and the results are summarized in Table 5. All the polymerizations proceeded smoothly, affording polymers with high *M*<sub>w</sub> (21 400–40 800) and low polydispersity (2.0–2.3) in high yields (95–99%). It is noteworthy that the polydispersity of the polymers obtained from this sequential polymerization is much smaller compared with the previously reported polymers prepared by similar MCTPs.<sup>14</sup>

### Model reaction

A model compound was also prepared to assist the structural characterization of the polymers (Scheme 5). TPE-containing monoyne **5** was first reacted with benzoyl chloride **6**, catalyzed by Pd(PPh<sub>3</sub>)<sub>2</sub>Cl<sub>2</sub>/CuI under nitrogen at room temperature for

**Scheme 5** Synthetic route to model compound **4**.**Fig. 1** (A) Single crystal structure (CCDC 1009262) and fluorescence images of **4** taken under a fluorescence microscope with an excitation light of (B) 330–385 nm, (C) 460–490 nm, and (D) 510–560 nm.

3 h. The reactive intermediate obtained from the first step then directly underwent the next *in situ* reaction at 80 °C after addition of **3a**, affording model compound **4**. To provide direct insight into the molecular structure, single crystals were obtained from the hexane/DCM solution of **4**. From the X-ray analysis shown in Fig. 1A and Table S1,<sup>†</sup> the *Z* isomer of the newly formed C=C bond was obtained exclusively with the formation of an intramolecular hydrogen bond between N–H and O=C groups. In addition, the crystals are observed to emit green, yellow and red fluorescence under UV, blue, and green light irradiation of the fluorescence microscope, respectively (Fig. 1B–D). Upon irradiation with different excitation lights, the emission light with a wavelength smaller than the excitation light wavelength was eliminated by specific filters. Hence a different fluorescence of model compound **4** was observed.

### Structural characterization

All the monomers, model compounds and polymers were characterized by standard spectroscopic techniques, which provided satisfactory analysis data corresponding to the expected molecular structures (see the Experimental section). For example, the IR spectra of **1a**, **2**, **3a**, **4** and **P1a/2/3a** are shown in Fig. 2 for comparison. The absorption bands of **1a** associated with ≡C–H and C≡C stretching vibrations were located at 3275 and 2106 cm<sup>-1</sup>, respectively. Meanwhile, an absorption band with double peaks in the IR spectrum of **3a** was observed at 3348 and 3279 cm<sup>-1</sup>, which was associated with the NH<sub>2</sub> stretching vibration. The bands disappeared in the spectra of both **4** and **P1a/2/3a**, confirming that the terminal triple bonds and NH<sub>2</sub> groups have been completely consumed by the reaction.

Furthermore, their <sup>1</sup>H NMR spectra are compared in Fig. 3. The resonances of the acetylene protons of **1a** at δ 3.03 dis-



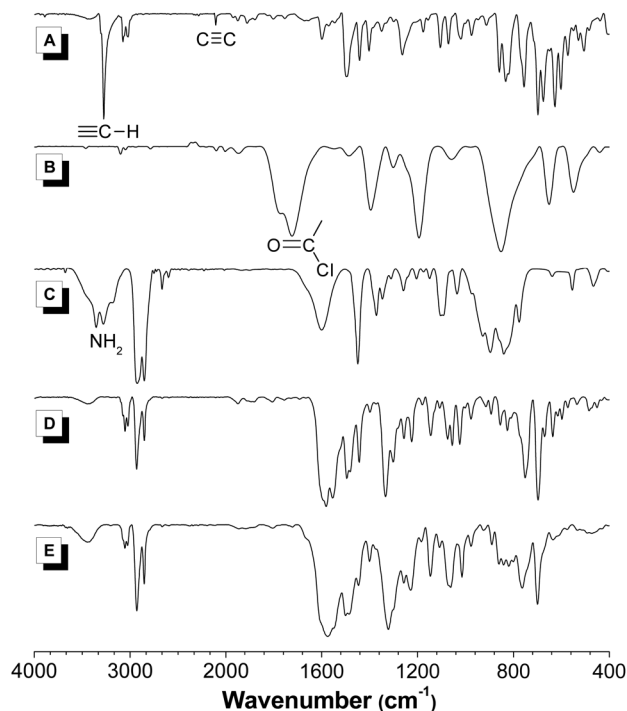


Fig. 2 IR spectra of (A) 1a, (B) 2, (C) 3a, (D) 4 and (E) P1a/2/3a.

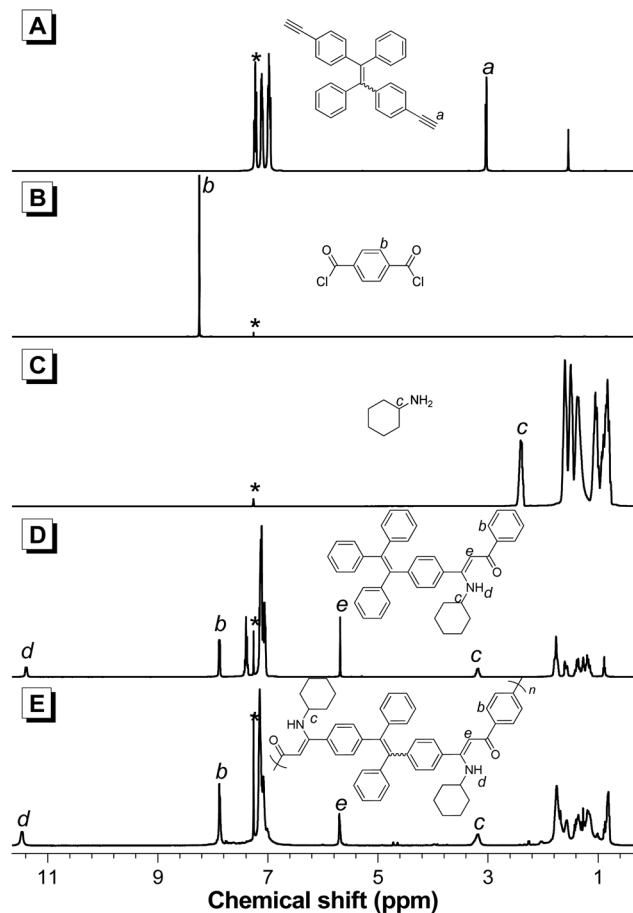


Fig. 3 <sup>1</sup>H NMR spectra of (A) 1a, (B) 2, (C) 3a, (D) 4 and (E) P1a/2/3a.

appeared in the spectra of 4 and P1a/2/3a. The resonances of the aromatic protons of 2 at  $\delta$  8.25 and the CH proton of 3 next to the NH<sub>2</sub> group at  $\delta$  2.40 shifted to  $\delta$  7.87 and  $\delta$  3.19, respectively, in the model compound and polymer after the reaction. On the other hand, new peaks emerged at  $\delta$  5.69 and  $\delta$  11.40 in the spectra of both 4 and P1a/2/3a, representing the newly formed C=CH group next to the carbonyl group, and the N-H group, respectively. The N-H resonance was located at a low field, indicating the formation of an intramolecular hydrogen bond. Generally, the resonance peaks of P1a/2/3a are broader than those of 4, suggesting its polymeric nature. Similarly, in the <sup>13</sup>C NMR spectra, the resonances of C≡C-H of 1 at  $\delta$  83.9 and 77.7 were absent in the spectra of 4 and P1a/2/3a (Fig. 4). The absorption of the carbonyl group of 2 at  $\delta$  170.8 was shifted to  $\delta$  188.1 after the reaction. In the spectra of 4 and P1a/2/3a, two new peaks emerged at  $\delta$  166.1 and 93.4, which were associated with the =C<sub>Ar</sub>(N) and =CH(COAr) olefin carbons, respectively. In addition, the newly formed olefin group was confirmed to be a *Z*-isomer in 4 by X-ray single crystal structure analysis. From the above discussed <sup>1</sup>H/<sup>13</sup>C NMR spectra, P1a/2/3a shares exactly the same NMR spectral pattern with 4, without any additional peaks observed for the *E*-isomer, proving its highly regio- and stereospecific structure as shown in Scheme 4.

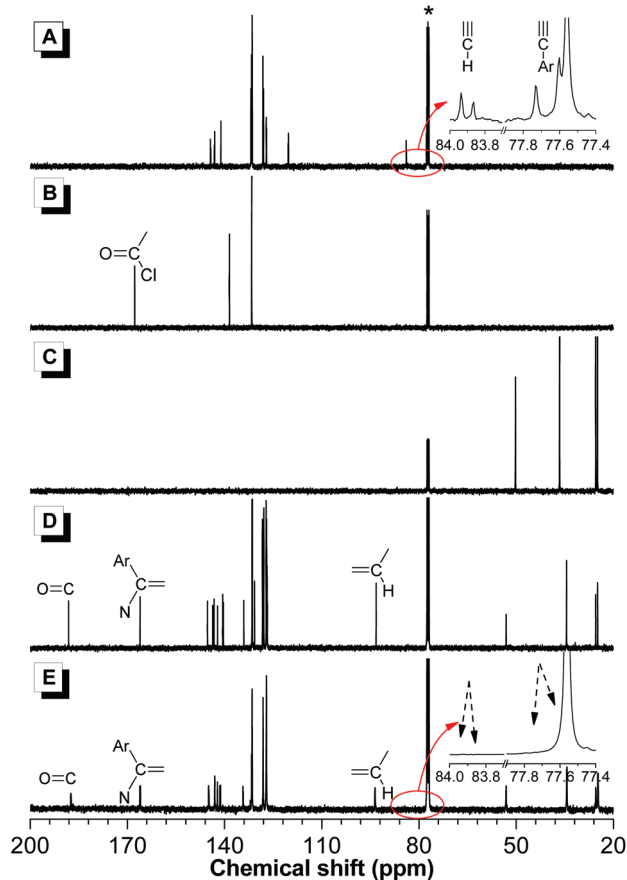


Fig. 4 <sup>13</sup>C NMR spectra of (A) 1a, (B) 2, (C) 3a, (D) 4 and (E) P1a/2/3a.

### Solubility and thermal stability

Although the resulting polymers are composed of conjugated aromatic backbones, they possess good solubility in common organic solvents, such as THF, DCM, chloroform, *etc.* The introduction of TPE units into the polymer backbone played a major role in improving the solubility, owing to the bulky and twisted structure of TPE units, which may result in large intermolecular distance and hence provide free volume for solvent molecules. Moreover, the polymers generally possess good film-forming ability and can be readily fabricated into thin films by the spin-coating process. With their conjugated polymer backbones and aromatic components, the polymers enjoy good thermal stability. Their thermal properties were evaluated by thermogravimetric analysis, indicating that the degradation temperatures ( $T_d$ ) of P1a-b/2/3a-b at their 5% weight losses under nitrogen were in the range of 318–351 °C (Fig. 5).

### Photophysical properties

With the typical AIE-active TPE units embedded in the molecular skeletons, AIE or AEE characteristics can be expected for both model compounds and the corresponding polymers. The photophysical properties of **4** and P1a/2/3a were hence systematically investigated. The absorption spectra of **4** and P1a/2/3a in pure THF solutions with a concentration of 10  $\mu\text{M}$  were firstly measured as shown in Fig. 6. The absorption maxima of **4** and P1a/2/3a were located at 355 and 387 nm, respectively, indicating better conjugation in the polymer.

Both polymers and model compounds are comprised of TPE as the fluorophore, which is linked with amine moieties, representing a typical photo-induced electron transfer (PET) system (Fig. S1†).<sup>20</sup> In the general PET process, when the fluorophore is irradiated, the electron on the highest occupied molecular orbital (HOMO) is excited to the lowest unoccupied molecular orbital (LUMO). If the HOMO level of the amine moiety with lone pair electrons is located between the LUMO

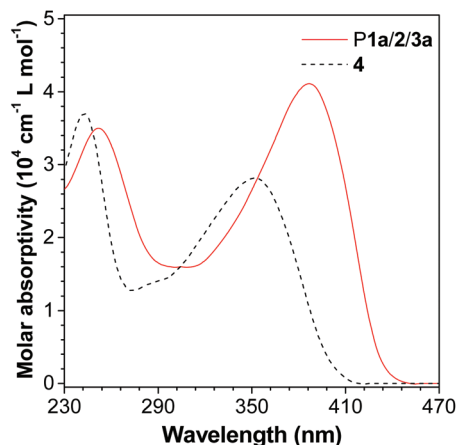


Fig. 6 Absorption spectra of **4** and P1a/2/3a in THF solutions. Solution concentration: 10  $\mu\text{M}$ .

and HOMO levels of the adjacent fluorophores, the electron on the HOMO level of the amine will be easily transferred to the HOMO level of the fluorophores. Such a process hinders the return of the electron on the LUMO level of the fluorophores to its HOMO level, and hence causes fluorescence quenching.<sup>21</sup> However, in **4** and P1a/2/3a, the potential PET process was blocked by the intramolecular hydrogen bond, rendering the fluorophores emissive.

The photoluminescence (PL) of both **4** and P1a/2/3a was estimated by using a spectrofluorometer (Fig. 7 and 8). The THF solution of **4** was weakly emissive with a flat peak at 460 nm in its PL spectrum. The emission intensity slowly increased with the addition of water, a poor solvent of **4**, until 70 vol% of water was added. Eventually, the emission intensity increased by 8.9-fold when nanoaggregates formed in the THF/water mixture with 99 vol% water content and the emission peak was red-shifted to 500 nm. The emission maximum of P1a/2/3a in THF solution was located at 536 nm, bathochromi-

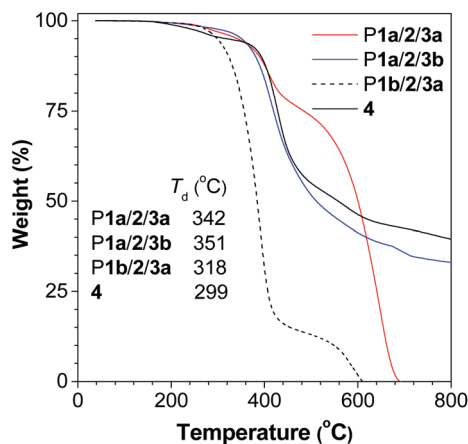


Fig. 5 TGA thermograms of **4** and P1a-b/2/3a-b recorded under nitrogen at a heating rate of 10  $^{\circ}\text{C min}^{-1}$ .

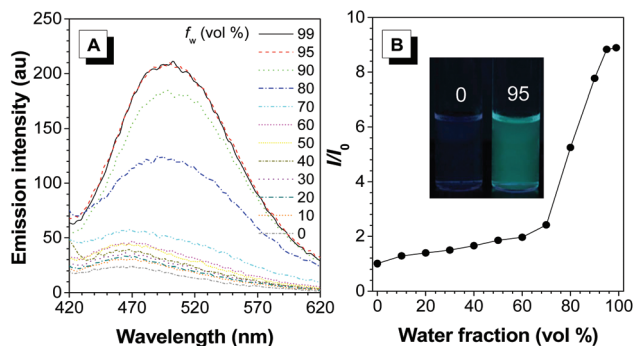
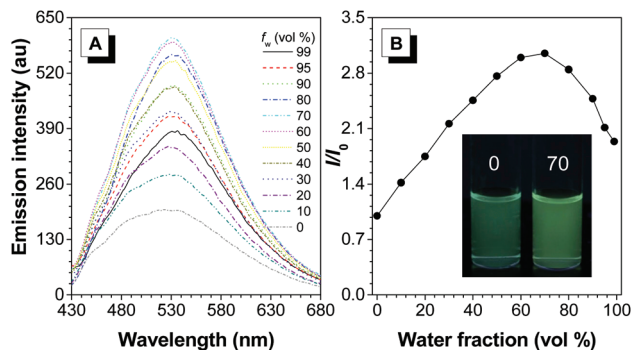


Fig. 7 (A) Emission spectra of **4** in THF/water mixtures with different water fractions ( $f_w$ ). (B) Plot of relative emission intensity ( $I/I_0$ ) versus the water fraction of the aqueous mixtures of **4**. Inset: fluorescence photographs of **4** in THF solution and 95% aqueous mixture taken under 365 nm UV irradiation. Solution concentration: 10  $\mu\text{M}$ ; excitation wavelength: 355 nm.



**Fig. 8** (A) Emission spectra of P1a/2/3a in THF/water mixtures with different water fractions ( $f_w$ ). (B) Plot of relative emission intensity ( $I/I_0$ ) versus the water fraction of the aqueous mixtures of P1a/2/3a. Inset: fluorescence photographs of P1a/2/3a in THF solution and 70% aqueous mixture taken under 365 nm UV irradiation. Solution concentration: 10  $\mu$ M; excitation wavelength: 387 nm.

cally shifted about 76 nm compared with that of **4**. In contrast to the small molecule, the fluorophores of the polymer were covalently-linked in the polymer backbone, which partially restricted the free rotation of the phenyl rings to some extent in the solution. Thus the THF solution of P1a/2/3a was faintly emissive. The continuous addition of water into the THF solution of P1a/2/3a with a constant concentration of 10  $\mu$ M gradually enhanced its emission intensity without a noticeable shift in the emission peak. The highest emission intensity was observed in the THF/water mixture with 70 vol% water and its intensity was about 3.0-fold higher than that of its THF solution, demonstrating aggregation-enhanced emission characteristics. When more water was added, the emission intensity decreased because of the poor solubility of P1a/2/3a in the aqueous mixtures.

The fluorescence photographs of **4** and P1a/2/3a in THF and THF/water mixtures are displayed in the insets of Fig. 7B and 8B. With an identical dye concentration, the THF solution of **4** was almost non-emissive and the nanoaggregates formed in the THF/water mixture with 95 vol% water fraction were brightly emissive under UV irradiation. Similarly, the nanoaggregates of P1a/2/3a formed in the THF/water mixture are more emissive compared with their THF solution. The PL study suggested that the formation of intramolecular hydrogen bonds prevented the electron transfer from the HOMO level of the amine group to the HOMO level of the TPE fluorophores. The quantum yields of **4** and P1a-b/2/3a-b were also measured in the solution and aggregate state, respectively. The detailed information is summarized in Table S2,<sup>†</sup> which further demonstrates their AIE and AEE characteristics.

### Light refraction

Processable macromolecules with high refractive indices ( $n$ ) are promising candidates due to a variety of practical applications in advanced optoelectronic fabrications, such as lenses, prisms, substrates for advanced display devices, optical

adhesives of organic light-emitting diode devices, and micro-lens components for charge coupled devices or complementary metal oxides, *etc.*<sup>22</sup> Generally, conventional organic polymer materials including polystyrenes, poly(methyl-methacrylate)s, and polycarbonates possess refractive indices in the region of 1.49–1.58.<sup>23</sup> Usually, polymer materials with a large number of well-known contributors for increasing refractivity such as carbonyl groups, heteroatoms, and aromatic rings can be expected to display high refractivity. Polymers P1a-b/2/3a-b comprised plenty of carbonyl groups, heteroatoms, TPE moieties, and a conjugated polymer backbone. Hence, the thin films of P1a/2/3a, P1a/2/3b, and P1b/2/3a fabricated through the spin-coating process exhibited high  $n$  values of 1.9103–1.6582, 1.9758–1.6501, and 2.0182–1.6403 in a wide spectral region of 400–1000 nm, respectively (Fig. 9A). Such high refractivity is presumably derived from both the special polymer structure and the TPE building blocks.

Modulation of the refractive index is another critical technology in optical communication and optical data storage devices such as compact discs, digital versatile discs, blue ray discs, holographic recording materials, *etc.*<sup>24</sup> Therefore, it is of great importance to develop materials with high and facilely tunable refractive indices. P1a/2/3a was investigated as an example and the changes in the  $n$  values of its thin film with different UV irradiation times are shown in Fig. 9B. When UV irradiation was applied on the polymer thin film in air, photo-oxidation reaction occurred, which changed the chemical composites of the film and hence the  $n$  values. The  $n$  values dropped quickly in the same wavelength region upon the exposure of UV light. Particularly, after 30 min UV irradiation, the  $n$  values of the film decreased to 1.6746–1.5590 in the wavelength region of 400–1000 nm, and the difference of the  $n$  value was about 0.1204 at 632.0 nm, demonstrating efficient refractivity modulation.

### Fluorescent photopatterning

It is highly desirable to fabricate fluorescent photopatterns for the construction of photonic and electronic devices, and biological sensing and probing systems.<sup>25</sup> Since the polymers exhibit good film-forming ability, photosensitivity, and high

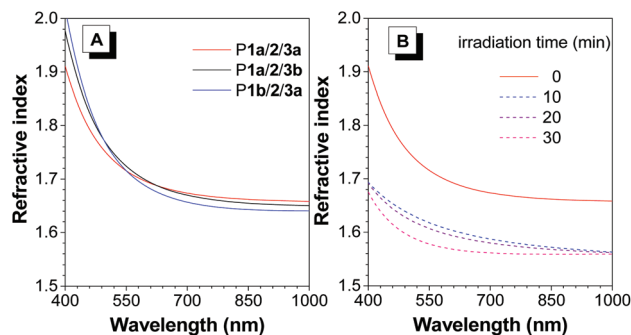


**Fig. 9** Wavelength dependence of refractive indices of thin films of (A) P1a-b/2/3a-b and (B) P1a/2/3a with different UV irradiation times.

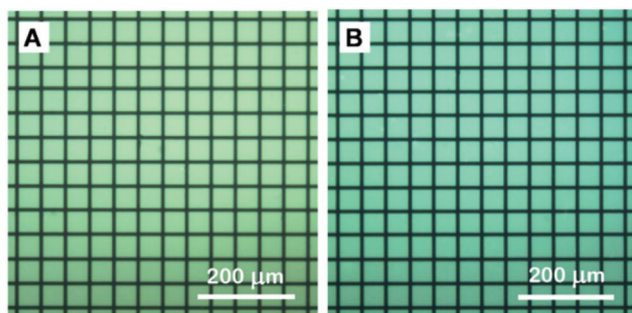


**Fig. 10** Two-dimensional fluorescent photopatterns generated by photo-oxidation of thin films of (A) P1a/2/3a and (B) P1a/2/3b. The photographs were taken under UV light illumination (330–385 nm).

emission efficiency in the solid state, it is of great potential to fabricate them into luminescent photopatterns through photolithography. P1a/2/3a and P1a/2/3b were dissolved in 1,2-dichloroethane, to form emissive thin films on silicon wafers by spin-coating. Afterwards, the films were irradiated under UV light through a copper photomask for 20 min and two-dimensional patterns with high resolution and sharp edges were observed under a fluorescence microscope (Fig. 10). The fluorescence of the exposed region was quenched due to the photo-oxidation reaction in air.

## Conclusions

In this work, we have reported an efficient one-pot coupling-hydroamination polymerization of alkynes, carbonyl chlorides, and primary amines. The one-pot sequential Sonogashira coupling of the alkyne and carbonyl chloride, and hydroamination of the internal alkyne proceeded smoothly under mild conditions, furnishing nitrogen-containing conjugated polymers with high regioselectivity and stereoselectivity, and high molecular weights in excellent yields. Through the design of intramolecular hydrogen bond formation between N–H and C=O groups in the product, 100% stereoselectivity of the newly formed olefin groups was achieved. Moreover, benefited by the hydrogen bond-bound six membered ring, the *Z*-isomer was stabilized, the transformation between *Z*-vinylene and *E*-vinylene was blocked, and the enamine–imine tautomerization was inhibited. Most importantly, the intramolecular hydrogen bonds hampered the potential PET process and enabled the polymers to show aggregation-enhanced emission behaviors. The well-defined conjugated polymers enjoyed good solubility in common organic solvents, excellent film-forming ability, high thermal stability, large and tunable refractivity, photosensitivity, *etc.*

Through this efficient and convenient one-pot tandem polymerization approach towards functional conjugated polymer materials, polyhydroamination can be realized, overcoming the perennial problems such as low efficiency, unstable product structure, poor regioselectivity and stereo-

selectivity, and tautomerization. We believe that the general applicability of such an efficient approach will pave the way for the facile syntheses of heteroatom-containing conjugated polymers with well-defined structures and multiple functionalities.

## Experimental

### Materials and methods

THF was distilled from sodium benzophenone ketyl under a nitrogen atmosphere prior to use. Terephthaloyl dichloride and Et<sub>3</sub>N were purchased from Sigma-Aldrich. Pd(PPh<sub>3</sub>)<sub>2</sub>Cl<sub>2</sub>, CuI and methanol were ordered from Zhejiang Metallurgical Research Institute Co., Ltd, International Laboratory USA, and Merck, respectively. All of them were used as received without further purification except for special illustration. Dienes **1a–b** and monoyne **5** were prepared according to the literature procedures.<sup>19</sup>

<sup>1</sup>H and <sup>13</sup>C NMR spectra were recorded on a Bruker ARX 400 NMR spectrometer using CDCl<sub>3</sub> as the solvent and tetramethylsilane (TMS; δ = 0 ppm) as the internal standard. IR spectra were recorded on a Perkin-Elmer 16 PC FT-IR spectrophotometer. High resolution mass spectra (HRMS) were evaluated on a GCT Premier CAB 048 mass spectrometer operated in MALDI-TOF mode. Single crystal X-ray diffraction data were collected at 100 K on a Bruker-Nonius Smart Apex CCD diffractometer with graphite monochromated Mo-Kα radiation. Analysis of the data was carried out through the SAINT and SADABS routines, and the structure and refinement were obtained by employing the SHELTL suite of X-ray programs (version 6.10). The weight average molecular weights (*M<sub>w</sub>*), number average molecular weights (*M<sub>n</sub>*), and polydispersity indices (*M<sub>w</sub>/M<sub>n</sub>*) of the polymers were evaluated by a Waters Associates gel permeation chromatography (GPC) system equipped with a RI detector. Distilled THF was used as the solvent to dissolve the polymers (~2 mg mL<sup>-1</sup>). The solutions were filtered through 0.45 μm PTFE syringe-type filters before being injected into the GPC system, and THF was used as the eluent at a flow rate of 1.0 mL min<sup>-1</sup>. A set of linear polystyrene standards (Waters) covering the *M<sub>w</sub>* range of 10<sup>3</sup>–10<sup>7</sup> were utilized for *M<sub>w</sub>* and PDI calibration.

A Milton Roy Spectronic 3000 array spectrophotometer and a Perkin-Elmer LS 55 spectrofluorometer were utilized to record the UV-Vis absorption spectra and PL spectra, respectively. Quantum yields were determined by using a calibrated integrating sphere. TGA was carried out under nitrogen on a Perkin-Elmer TGA 7 analyzer with a heating rate of 10 °C min<sup>-1</sup>. Refractive indices were measured through a J. A. Woollam M-2000 V multi-wavelength ellipsometer from 400 nm to 1000 nm. Photopatterning and refractivity modulation of the polymer films were conducted on a Spectroline ENF-280C/F UV lamp as the light source at a distance of 3 cm with an incident light intensity of ~18.5 mW cm<sup>-2</sup>. The films were prepared by spin-coating of the polymer solutions (10 mg polymer in 1 mL 1,2-dichloroethane) at 1000 rpm for 1 min on silicon wafers. The films were dried in a vacuum oven at room



temperature overnight. The patterns were generated by UV irradiation on the film through a copper photomask for 20 min. All of the photos were taken under a UV light source by using an optical microscope (Olympus BX 41).

### Polymerizations

All the polymerizations were carried out under nitrogen using a standard Schlenk technique. A typical procedure for the synthesis of P1a/2/3a from Table 1, no. 3 is given below as an example. A 25 mL Schlenk tube equipped with a magnetic stirrer was placed with TPE-containing diyne 1a (76 mg, 0.20 mmol), terephthaloyl chloride 2 (41 mg, 0.20 mmol), Pd(PPh<sub>3</sub>)<sub>2</sub>Cl<sub>2</sub> (6 mg, 0.008 mmol), and CuI (3 mg, 0.016 mmol). The Schlenk tube was evacuated under vacuum and flushed with dry nitrogen three times. 3.5 mL of THF and 0.06 mL of Et<sub>3</sub>N were then injected and the resulting solution was stirred for 15 minutes at room temperature. Afterwards, cyclohexylamine 3a (0.10 mL, 0.80 mmol) was injected with 0.50 mL of methanol (THF/methanol = 7/1). The reaction mixture was stirred for 6 h at 80 °C under nitrogen and was then added dropwise into 200 mL of methanol *via* a cotton filter to precipitate. The precipitate was allowed to stand overnight and collected by filtration. The polymer was washed with methanol and dried under vacuum at room temperature to a constant weight.

**P1a/2/3a.** Yellow powder; 99% (Table 1, no. 3). *M<sub>w</sub>*: 40 800; *M<sub>w</sub>*/*M<sub>n</sub>*: 2.3 (GPC, polystyrene calibration). IR (KBr),  $\nu$  (cm<sup>-1</sup>): 3054, 3027, 2930, 2853, 1575, 1504, 1445, 1322, 1256, 1229. <sup>1</sup>H NMR (400 MHz, CDCl<sub>3</sub>),  $\delta$  (TMS, ppm): 11.47, 7.87, 7.15, 7.08, 5.69, 3.22, 1.75, 1.36, 1.15. <sup>13</sup>C NMR (100 MHz, CDCl<sub>3</sub>),  $\delta$  (TMS, ppm): 187.38, 166.17, 165.96, 144.93, 144.82, 143.04, 142.20, 141.43, 141.25, 134.36, 134.23, 131.65, 131.51, 128.11, 127.10, 93.60, 93.56, 53.16, 53.08, 34.45, 34.33, 25.46, 25.37, 24.83, 24.71.

**P1b/2/3a.** Yellow powder; 99% (Table 5, no. 2). *M<sub>w</sub>*: 21 400; *M<sub>w</sub>*/*M<sub>n</sub>*: 2.2 (GPC, polystyrene calibration). IR (KBr),  $\nu$  (cm<sup>-1</sup>): 3054, 3027, 2930, 2853, 1575, 1504, 1445, 1400, 1322, 1258. <sup>1</sup>H NMR (400 MHz, CDCl<sub>3</sub>),  $\delta$  (TMS, ppm): 11.49, 7.88, 7.15, 7.06, 5.71, 3.20, 1.76, 1.36, 1.20. <sup>13</sup>C NMR (100 MHz, CDCl<sub>3</sub>),  $\delta$  (TMS, ppm): 187.40, 166.11, 144.63, 143.25, 142.22, 139.53, 134.28, 131.58, 131.49, 127.99, 127.20, 127.08, 93.55, 53.15, 34.44, 25.46, 24.81.

**P1a/2/3b.** Yellow powder; 95% (Table 5, no. 3). *M<sub>w</sub>*: 25 200; *M<sub>w</sub>*/*M<sub>n</sub>*: 2.0 (GPC, polystyrene calibration). IR (KBr),  $\nu$  (cm<sup>-1</sup>): 3054, 3027, 2927, 2856, 1578, 1485, 1400, 1324, 1298, 1227. <sup>1</sup>H NMR (400 MHz, CDCl<sub>3</sub>),  $\delta$  (TMS, ppm): 11.43, 7.89, 7.15, 7.08, 5.73, 3.14, 1.53, 1.29, 0.88. <sup>13</sup>C NMR (100 MHz, CDCl<sub>3</sub>),  $\delta$  (TMS, ppm): 187.75, 167.15, 145.09, 144.98, 143.04, 142.26, 141.40, 133.91, 131.53, 128.12, 127.35, 127.24, 127.11, 93.49, 44.98, 31.55, 30.97, 26.61, 22.72, 22.67, 14.24, 14.21.

### Model reaction

(*Z*)-3-(Cyclohexylamino)-1-phenyl-3-(4-(1,2,2-triphenylvinyl)-phenyl)-prop-2-en-1-one (4): a 25 mL Schlenk tube equipped with a magnetic stirrer was charged with TPE-containing monoyne (5)

(178 mg, 0.50 mmol), benzoyl chloride (6) (0.06 mL, 0.50 mmol), Pd(PPh<sub>3</sub>)<sub>2</sub>Cl<sub>2</sub> (8 mg, 0.01 mmol), and CuI (4 mg, 0.02 mmol). 3.5 mL of THF and 0.08 mL of Et<sub>3</sub>N were injected under nitrogen and then stirred at room temperature for 3 h. Cyclohexylamine 3a (0.06 mL, 0.50 mmol) and 0.50 mL of methanol were injected subsequently by using a syringe. The reaction mixture was further stirred for 24 h at 80 °C under nitrogen. 20 mL of water was added to quench the reaction and the solution was extracted with 30 mL of DCM three times. The solvent was evaporated and the resulting crude product was purified by a silica-gel chromatography column using DCM/hexane (v/v 1/1) as the eluent to give a light yellow solid in 72% yield. IR (KBr),  $\nu$  (cm<sup>-1</sup>): 3051, 3025, 2931, 2851, 1581, 1496, 1443, 1333, 1300, 1256, 1225. <sup>1</sup>H NMR (400 MHz, CDCl<sub>3</sub>),  $\delta$  (TMS, ppm): 11.40 (d, *J* = 9.3 Hz, 1H), 7.88 (d, *J* = 6.4 Hz, 2H), 7.39 (m, 3H), 7.16–7.09 (m, 9H), 7.07–7.01 (m, 8H), 5.69 (s, 1H), 3.19 (d, *J* = 9.8 Hz, 1H), 1.77 (m, 4H), 1.38 (m, 2H), 1.21 (m, 4H). <sup>13</sup>C NMR (100 MHz, CDCl<sub>3</sub>),  $\delta$  (TMS, ppm): 188.12, 166.08, 145.27, 143.69, 143.42, 143.28, 142.19, 140.57, 140.36, 134.09, 131.56, 131.53, 131.48, 131.45, 130.74, 128.33, 128.03, 127.92, 127.89, 127.19, 127.04, 126.91, 126.89, 126.85, 93.25, 77.23, 53.11, 34.48, 25.49, 24.87. HRMS (MALDI-TOF): *m/z* 560.2910 [M + H<sup>+</sup>, calcd 560.2953].

### Preparation of nanoaggregates

Stock THF solutions of 4 and P1a/2/3a with a concentration of 1 mM were prepared. Then 0.10 mL of the stock solutions were transferred to 10.00 mL volumetric flasks. After addition of an appropriate amount of THF, water was added dropwise under vigorous stirring to prepare 10  $\mu$ M THF/water mixtures with water fractions (*f<sub>w</sub>*) of 0–99 vol%. The absorption and emission measurements of the resulting solutions were immediately performed.

## Acknowledgements

This work was partially supported by the National Basic Research Program of China (973 Program; 2013CB834701), the University Grants Committee of Hong Kong (AoE/P-03/08), the National Science Foundation of China (21490570 and 21490574), the Research Grants Council of Hong Kong (604913 and 602212), Science and Technology Plan of Shenzhen (JCYJ20140425170011516) and Natural Science Fund of Guangdong Province (2014A030313659). B. Z. Tang thanks the support of the Guangdong Innovative Research Team Program (201101C0105067115).

## Notes and references

- 1 P. C. Hiemenz and T. Lodge, *Polymer chemistry*, CRC Press, Boca Raton, 2007.
- 2 (a) H. Sirringhaus, T. Kawase, R. H. Friend, T. Shimoda, M. Inbasekaran, W. Wu and E. P. Woo, *Science*, 2000, **290**,

- 2123–2126; (b) D. T. McQuade, A. E. Pullen and T. M. Swager, *Chem. Rev.*, 2000, **100**, 2537–2574; (c) C. L. Wang, H. L. Dong, W. P. Hu, Y. Q. Liu and D. B. Zhu, *Chem. Rev.*, 2012, **112**, 2208–2267; (d) N. Wang, Z. Chen, W. Wei and Z. Jiang, *J. Am. Chem. Soc.*, 2013, **135**, 17060–17068; (e) Z. Chen, P. Cai, J. Chen, X. Liu, L. Zhang, L. Lan, J. Peng, Y. Ma and Y. Cao, *Adv. Mater.*, 2014, **26**, 2586–2591; (f) A. Facchetti, *Chem. Mater.*, 2011, **23**, 733–758.
- 3 (a) J. Z. Liu, J. W. Y. Lam and B. Z. Tang, *Chem. Rev.*, 2009, **109**, 5799–5867; (b) A. J. Qin, J. W. Y. Lam and B. Z. Tang, *Chem. Soc. Rev.*, 2010, **39**, 2522–2544; (c) J. W. Y. Lam and B. Z. Tang, *Acc. Chem. Res.*, 2005, **38**, 745–754; (d) K. Matyjaszewski and J. H. Xia, *Chem. Rev.*, 2001, **101**, 2921–2990; (e) N. V. Tsarevsky and K. Matyjaszewski, *Chem. Rev.*, 2007, **107**, 2270–2299; (f) N. Hadjichristidis, H. Iatrou, M. Pitsikalis and G. Sakellariou, *Chem. Rev.*, 2009, **109**, 5528–5578.
- 4 A. Molnar, A. Sarkany and M. Varga, *J. Mol. Catal. A: Chem.*, 2001, **173**, 185–221.
- 5 X. M. Zeng, *Chem. Rev.*, 2013, **113**, 6864–6900.
- 6 (a) P. Lu, J. W. Y. Lam, J. Liu, C. K. W. Jim, W. Yuan, C. Y. K. Chan, N. Xie, Q. Hu, K. K. L. Cheuk and B. Z. Tang, *Macromolecules*, 2011, **44**, 5977–5986; (b) P. Lu, J. W. Y. Lam, J. Z. Liu, C. K. W. Jim, W. Z. Yuan, N. Xie, Y. C. Zhong, Q. Hu, K. S. Wong, K. K. L. Cheuk and B. Z. Tang, *Macromol. Rapid Commun.*, 2010, **31**, 834–839; (c) Z. J. Zhao, T. Jiang, Y. J. Guo, L. Y. Ding, B. R. He, Z. F. Chang, J. W. Y. Lam, J. Z. Liu, C. Y. K. Chan, P. Lu, L. W. Xu, H. Y. Qiu and B. Z. Tang, *J. Polym. Sci., Part A: Polym. Chem.*, 2012, **50**, 2265–2274.
- 7 (a) J. Liu, J. W. Y. Lam, C. K. W. Jim, J. C. Y. Ng, J. Shi, H. Su, K. F. Yeung, Y. Hong, M. Faisal, Y. Yu, K. S. Wong and B. Z. Tang, *Macromolecules*, 2011, **44**, 68–79; (b) B. C. Yao, J. Z. Sun, A. J. Qin and B. Z. Tang, *Chin. Sci. Bull.*, 2013, **58**, 2711–2718.
- 8 (a) C. K. W. Jim, A. Qin, J. W. Y. Lam, F. Mahtab, Y. Yu and B. Z. Tang, *Adv. Funct. Mater.*, 2010, **20**, 1319–1328; (b) B. C. Yao, J. Mei, J. Li, J. Wang, H. Q. Wu, J. Z. Sun, A. J. Qin and B. Z. Tang, *Macromolecules*, 2014, **47**, 1325–1333.
- 9 (a) S. L. Shi and S. L. Buchwald, *Nat. Chem.*, 2015, **7**, 38–44; (b) F. Pohlki and S. Doye, *Chem. Soc. Rev.*, 2003, **32**, 104–114; (c) R. Severin and S. Doye, *Chem. Soc. Rev.*, 2007, **36**, 1407–1420; (d) T. E. Muller, K. C. Hultsch, M. Yus, F. Foubelo and M. Tada, *Chem. Rev.*, 2008, **108**, 3795–3892.
- 10 (a) M. L. Buil, M. A. Esteruelas, A. M. Lopez and A. C. Mateo, *Organometallics*, 2006, **25**, 4079–4089; (b) M. A. Esteruelas, A. M. Lopez, A. C. Mateo and E. Onate, *Organometallics*, 2006, **25**, 1448–1460; (c) N. T. Patil and V. Singh, *J. Organomet. Chem.*, 2011, **696**, 419–432.
- 11 (a) Y. Z. Wang, X. X. Deng, L. Li, Z. L. Li, F. S. Du and Z. C. Li, *Polym. Chem.*, 2013, **4**, 444–448; (b) X. X. Deng, Y. Cui, F. S. Du and Z. C. Li, *Polym. Chem.*, 2014, **5**, 3316–3320; (c) A. Sehlinger, P. K. Dannecker, O. Kreye and M. A. R. Meier, *Macromolecules*, 2014, **47**, 2774–2783.
- 12 C. Y. K. Chan, N. W. Tseng, J. W. Y. Lam, J. Z. Liu, R. T. K. Kwok and B. Z. Tang, *Macromolecules*, 2013, **46**, 3246–3256.
- 13 (a) I. H. Lee, H. Kim and T. L. Choi, *J. Am. Chem. Soc.*, 2013, **135**, 3760–3763; (b) H. Kim and T. L. Choi, *ACS Macro Lett.*, 2014, **3**, 791–794.
- 14 H. Q. Deng, R. R. Hu, E. G. Zhao, C. Y. K. Chan, J. W. Y. Lam and B. Z. Tang, *Macromolecules*, 2014, **47**, 4920–4929.
- 15 C. Zheng, H. Q. Deng, Z. J. Zhao, A. J. Qin, R. R. Hu and B. Z. Tang, *Macromolecules*, 2015, **48**, 1941–1951.
- 16 A. S. Karpov and T. J. J. Müller, *Synthesis*, 2003, 2815–2826.
- 17 (a) Y. N. Hong, J. W. Y. Lam and B. Z. Tang, *Chem. Commun.*, 2009, 4332–4353; (b) R. Hu, N. L. Leung and B. Z. Tang, *Chem. Soc. Rev.*, 2014, **43**, 4494–4562.
- 18 (a) B. Z. Tang and A. Qin, *Aggregation-induced emission: fundamentals*, 2013; (b) Y. N. Hong, J. W. Y. Lam and B. Z. Tang, *Chem. Soc. Rev.*, 2011, **40**, 5361–5388; (c) J. Mei, Y. Hong, J. W. Lam, A. Qin, Y. Tang and B. Z. Tang, *Adv. Mater.*, 2014, **26**, 5429–5479; (d) J. D. Luo, Z. L. Xie, J. W. Y. Lam, L. Cheng, H. Y. Chen, C. F. Qiu, H. S. Kwok, X. W. Zhan, Y. Q. Liu, D. B. Zhu and B. Z. Tang, *Chem. Commun.*, 2001, 1740–1741.
- 19 (a) R. Hu, J. L. Maldonado, M. Rodriguez, C. Deng, C. K. W. Jim, J. W. Y. Lam, M. M. F. Yuen, G. Ramos-Ortiz and B. Z. Tang, *J. Mater. Chem.*, 2012, **22**, 232–240; (b) R. Hu, J. W. Y. Lam, M. Li, H. Q. Deng, J. Li and B. Z. Tang, *J. Polym. Sci., Part A: Polym. Chem.*, 2013, **51**, 4752–4764; (c) Y. J. Liu, M. Gao, J. W. Y. Lam, R. R. Hu and B. Z. Tang, *Macromolecules*, 2014, **47**, 4908–4919.
- 20 M. T. Z. Spence and I. D. Johnson, *The molecular probes handbook: a guide to fluorescent probes and labeling technologies*, Live Technologies Corporation, Carlsbad, CA, 2010.
- 21 (a) W. Zhang, Z. Ma, L. Du and M. Li, *Analyst*, 2014, **139**, 2641–2649; (b) A. P. de Silva, T. S. Moody and G. D. Wright, *Analyst*, 2009, **134**, 2385–2393.
- 22 (a) T. Nakamura, H. Fujii, N. Juni and N. Tsutsumi, *Opt. Rev.*, 2006, **13**, 104–110; (b) J. L. Regolini, D. Benoit and P. Morin, *Microelectron. Reliab.*, 2007, **47**, 739–742; (c) D. W. Mosley, K. Auld, D. Conner, J. Gregory, X. Q. Liu, A. Pedicini, D. Thorsen, M. Wills, G. Khanarian and E. S. Simon, *Proc. SPIE*, 2008, **6910**, 691017–691018; (d) J. Liu and M. Ueda, *J. Mater. Chem.*, 2009, **19**, 8907–8919.
- 23 (a) J. Brandrup, E. H. Immergut and E. A. Grulke, *Polymer handbook*, Wiley, New York, Chichester, 4th edn, 2004; (b) J. E. Mark, *Polymer data handbook*, Oxford University Press, Oxford, New York, 2009.
- 24 (a) H. G. Unger, *Planar optical waveguides and fibres*, Clarendon Press, Oxford Eng., New York, 1977; (b) V. V. Krongauz and A. D. Trifunac, *Processes in photoreactive polymers*, Chapman & Hall, New York, 1995; (c) T. Griesser, T. Höfler, G. Jakopic, M. Belzik, W. Kern and G. Trimmel, *J. Mater. Chem.*, 2009, **19**, 4557–4565; (d) M. Edler, S. Mayrbrugger, A. Fian, G. Trimmel, S. Radl, W. Kern and T. Griesser, *J. Mater. Chem. C*, 2013, **1**, 3931–3938.

- 25 (a) M. Irie, T. Fukaminato, T. Sasaki, N. Tamai and T. Kawai, *Nature*, 2002, **420**, 759–760; (b) R. Ando, H. Mizuno and A. Miyawaki, *Science*, 2004, **306**, 1370–1373; (c) J. M. Kim, Y. B. Lee, D. H. Yang, J. S. Lee, G. S. Lee and D. J. Ahn, *J. Am. Chem. Soc.*, 2005, **127**, 17580–17581; (d) S. J. Lim, J. Seo and S. Y. Park, *J. Am. Chem. Soc.*, 2006, **128**, 14542–14547; (e) M. S. Hahn, J. S. Miller and J. L. West, *Adv. Mater.*, 2006, **18**, 2679–2684; (f) J. M. Kim, *Macromol. Rapid Commun.*, 2007, **28**, 1191–1212; (g) Z. a. Li, Z. Jiang, S. Ye, C. K. W. Jim, G. Yu, Y. Liu, J. Qin, B. Z. Tang and Z. Li, *J. Mater. Chem.*, 2011, **21**, 14663–14671.